J Plant Growth Regul (2000) 19:98–105
DOI: 10.1007/s003440000010

J P G R
Journal of Plant Growth Regulation

The Double-Water-Film Electrode: A Device for Measuring the Resistance and the Capacitance of the Internode/Node Interface of *Chara* as Functions of Time and Temperature

Koreaki Ogata

School of Health Sciences, University of Occupational and Environmental Health, 1-1 Iseigaoka, Yahatanishiku, 807-8555 Fukuoka, Japan

Abstract

A "double-water-film electrode technique" has been developed for the long-term characterization of the electrical properties across the interface between the nodal (N) and internodal (A or B) cells and the vacuole along the length of an internode of *Chara* as a function of time and temperature. The electrode unit consisted of a pair of the water-film electrodes described elsewhere (Chilcott 1988; Chilcott and others 1983; Coster and others 1984; Lucas 1985; and Ogata 1983). The distance between two water-film probes was fixed at 1.0 cm. By scanning the electrode unit, the spatial variations in electrical resistance and capacitance along the longitudinal axis of *Chara* were observed. Analysis was performed by applying an electrical equivalent circuit for the biomembrane (Philippson 1921). Across the internode (−A or −B)/central nodal cells interface, the specific parallel resistance (Rm) and the parallel capacitance (Cm) at 20°C were $30 \pm 5 \times 10^{-3}$ Ωm^2 and $1.5 \pm 0.5 \times 10^{-1} Fm^{-2}$ (at 30 Hz), respectively. And the series resistance, corresponding to the vacuole of the internode was 8×10^{-3} Ωm^2. Study of temperature dependencies of Rm and Cm suggested that a dynamic homeostatic regulation was operating at the interface where numerous plasmodesmata were observed with an electron microscope (Pickett-Heaps 1967; Spanswick and Costerton 1967). Assuming that the individual cylinder of plasmodesma was filled only with cytoplasm, the number of plasmodesma per interface was estimated at 2.6×10^5.

Key words: Double-water-film-electrode; *Chara*; Plasmodesma(ta); Electrical properties; Homeostatic control; Intercellular communication.

Introduction

Single-cell organisms communicate with each other through the air and/or aqueous environments. Needless to say, these communications must be interrupted by unfavorable signals so that neither accurate nor rapid exchanges of information should be expected. Individual cells in a multicellular organism overcome these difficulties by junctions between adjacent cells. In the plant system, for ex-

Received 19 January 2000; accepted 16 March 2000
Corresponding author; e-mail: kor-ogat@health.uoeh-u.ac.jp

ample, a plasmodesma plays an important role as a gate for intercellular communication by passive diffusion of not only water and small solutes, small inorganic and organic substances, but also of many kinds of macromolecules, polysaccharides and even proteins. In fact, using a micromanometer developed to study growth rate in relation to turgor pressure of a young internode of *Nitella* (order, Charales), it has been shown that at least three adjacent internodes were required to obtain a sufficient growth rate in culture medium. The young internode required a sufficient supply of nutrition from neighboring internodes through the intercellular junctions (Green 1968).

To study the electrical conductivity at the node of *Chara,* many techniques have been used. Impaling conventional glass micropipette electrodes into the vacuole or the cytoplasm, specific resistances for the transnodal and/or across the node/internode-interface of *Chara* were found to be around 25 × 10^{-3} Ωm^2 (Bostrom and others 1975; Côté and others 1986; Ding and Tazawa 1989; Shibaoka 1981). With an extracellular four terminal measurement, values of spesitic parallel resistance (Rm) were up to 50 times smaller than those of plasmalemma and values of spesitic parallel capacitance (Cm) of 2 × $10^{-1}Fm^{-2}$ (1–100 Hz) were observed across the nodal complex of *Chara* (Chilcott and others 1993). To estimate the effective size of plasmodesmata openings, fluorescein-labeled macromolecules of various sizes were injected into the cytoplasm of *Nitella.* Molecules with a molecular weight as large as 20 kD were transported between internodes (Kikuyama and others 1992). On the other hand, a plasmodesma also operates as a sphincter (for example, in the case of rapid changes in environmental conditions, the electrical conductivity tends to decrease [Côté and others 1986; Ding and Tazawa 1989] and is thought to act as a defense). With electron microscopy, it was suggested that the diameter and length of the plasmodesma cylinder are 6 × 10^{-8} and 2 × 10^{-6} m, respectively (Spanswick and Costerton 1967). Furthermore, there was no evidence of any membranous structure in the inner space of *Chara* plasmodesmata (Franceshi and Lucas 1982). Other information on the structure and functions of plasmodesma have been reviewed in detail elsewhere (Robards and Lucas 1990).

The double-water-film electrode technique introduced here enabled us to observe the spatial variations of Rm, Cm, and series resistance (Rs) inside the material as a function of time, with negligible mechanical disturbance. Showing the dynamic response of these parameters to temperature change, the physiologic function and the size of plasmodesmata of *Chara* are discussed.

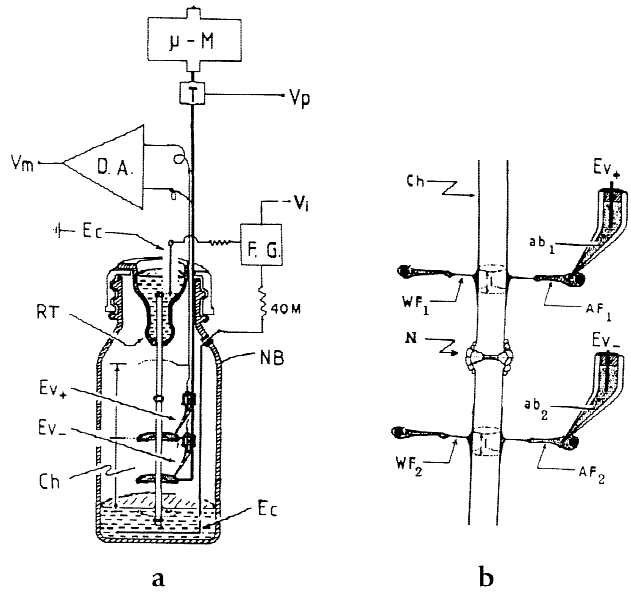

Figure 1. Schematic diagram of the double-water-film electrode. **(a)** Whole apparatus; **(b)** water-film probes in contact with the surface of *Chara;* μM, motor; Vp, output of potential monitoring the position of the electrode unit along the length of *Chara;* Vm, output of potential difference between Ev_{+and-}; DA, differential amplifier; Vi, output of potential monitoring the current given between Ecs; FG, function generator; RT, silicone rubber teat; $E_{V\pm}$, electrodes for the potential measurement; NB, nursing bottle; Ch, *Chara;* Ecs, electrodes for the current injection; $WF_{1,2}$, water-films; $AF_{1,2}$, agar-films; $ab_{1,2}$, agar-bridges; ls, effective length of potential measurement, and N, nodal complex joining two internodes.

Materials and Methods

The setup used for the newly developed double-water-film electrode is shown schematically in Figure 1a. The plant material, two internodes A and B of *Chara* joined by a nodal-complex, is inserted through a small hole in the tip of a silicone rubber teat. The pair of internodes is thus suspended in a water-saturated chamber, a nursing bottle, with about 5 mm of one end of the material submerged in artificial pond water (APW; contains 0.1 mM NaCl, 0.05 mM K_2SO_4, 1.0 mM $CaCO_3$ and buffered pH at 8.0 with 5.0 mM HEPES/$NaHCO_3$). The upper pool, the silicone rubber teat, is filled with APW. Two Ag/AgCl wire loops 1.0 cm each in diameter surround the axis of the material. The pair of loops, the double-water-film electrode-unit, can be moved up and down along the length of the material by the

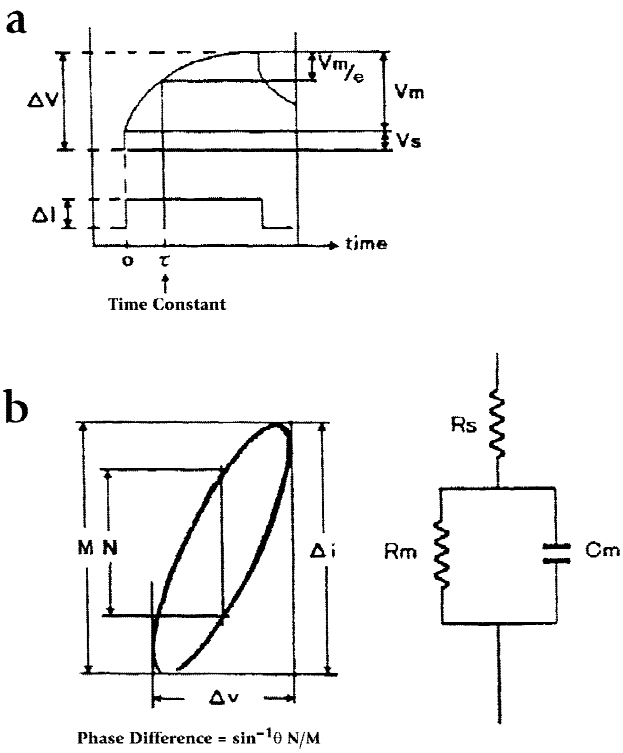

Figure 2. **(a)** Typical traces of oscilloscope recordings of potential change response to constant symmetric square current and **(b)** current/voltage ellipse and the respective electrical equivalent circuit. ΔI and Δi, maximum current injected between upper and lower-ends of material; Vm and Δv, maximum changes in voltage derived from the parallel resistance (Rm); Vs, potential change derived from the series resistance (Rs); ΔV = Vm + Vs; τ, time constant equal to Rm × Cm. The phase difference between Δi and Δv can be calculated with M (= Δi, the amplitude of the injected sinusoidal current) and N by the equation: $\sin^{-1}(N/M)$.

micromanipulator driven by an automatically controlled DC motor. Accurate position of the unit is monitored with a potentiometer (10 kΩ) that is directly connected to the micromanipulator with a universal joint. Each loop is coated with 3% of agar to stabilize not only the electrochemical potential of Ag/AgCl wire in the agar-bridge, but also the water-films that are formed by dipping both loops in APW containing 0.02% each of Tween-80, a detergent, and methylcellulose-4000 to prolong the life of the water-film in the moist chamber. When the loops are moved up and out of the solution, the water films remain. Thus, the electricity makes contact between each loop of the electrode unit and at two different places 1.0 cm apart along the surface of material (Figure 1b). The electrical potential measurements between the probes were made with a

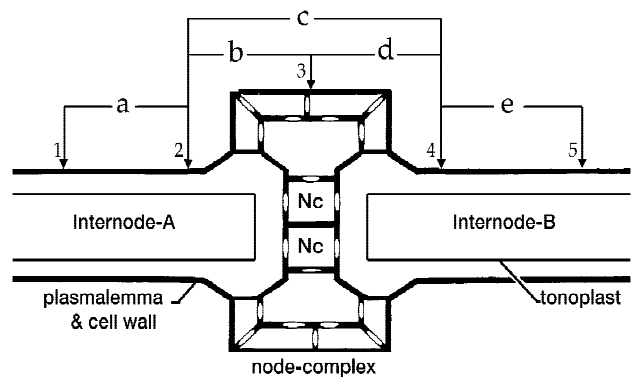

Figure 3. Schematic diagram of the longitudinal section around the node complex. Internodal cells A and B are joined by a pair of central nodal cells, Nc. *Arrows 1–5* indicate the positions of the water-films probing the respective potentials along the surface of material. *a, b, c, d,* and *e* indicate the potential differences between *1* & *2*, *2* & *3*, *2* & *4*, *3* & *4*, and *4* & *5*, respectively. For example, "*a*" measures the potential difference between *1* and *2* (one of the water-films, WF_1, is at position *1* and another, WF_2, is at position *2*). Bold lines are cell wall with the plasmalemma. The cytoplasmic connections corresponding to plasmodesmata are the open interruptions along the bold lines at the interfaces between two cells.

differential amplifier with $10^{14}\Omega$ of input impedance.

Injecting a symmetric-square or symmetric-sinusoidal constant electrical current (ΔI, 30 Hz, 4×10^{-7} amps, by means of a 40 M Ω -resistor) between the regions of internode A partly submerged in the upper pool and of internode B partly submerged in the lower pool, and scanning of the unit along the material enabled us to visualize the spatial variations of Rm, Rs, and Cm along the length of the material as functions of time. Rm is supposed to be the total electrical resistive component across the node/internode interface; Rs is supposed to be the total resistance of the vacuole and the cytoplasm; and Cm is supposed to be the total capacitative component across the node/internode interface (Figure 2). Assuming the electrical equivalent circuit shown in Figure 2a and injecting a constant symmetric square current, the specific values of each parameter Rm, Rs, and Cm can be calculated by the following equations;

$$Rm = Vm_{max}/I \times S \text{ (S is the effective area the current crosses)} \quad (1)$$

$$Rs = Vs_{max}/I \times S \quad (2)$$

$$Cm = \tau/Rm \text{ (}\tau\text{ is the time constant of } \Delta Vm) \quad (3)$$

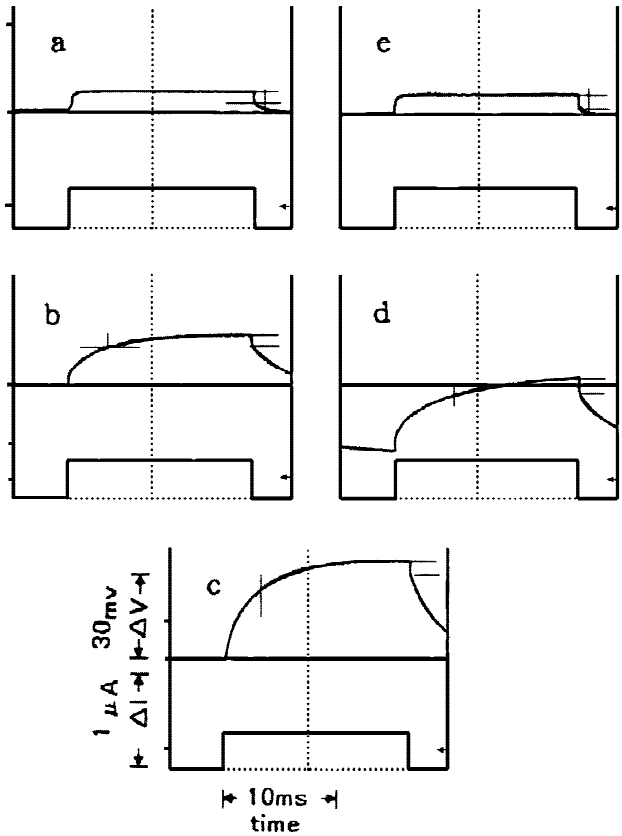

Figure 4. Typical potential responses at positions **a, b, c, d,** and **e,** resulting from the symmetric square currents (30 Hz, 4×10^{-7} amps, including a fast time constant of less than 0.5 ms) as a function of time. At positions **a** and **e,** only series resistance, Rs, can be observed. No significant difference in Rs can be seen among these recordings. The parallel resistance at position **c** (Rm *c*) roughly equals the sum of those at positions **b** and **d**. The axes scales are given in **c**.

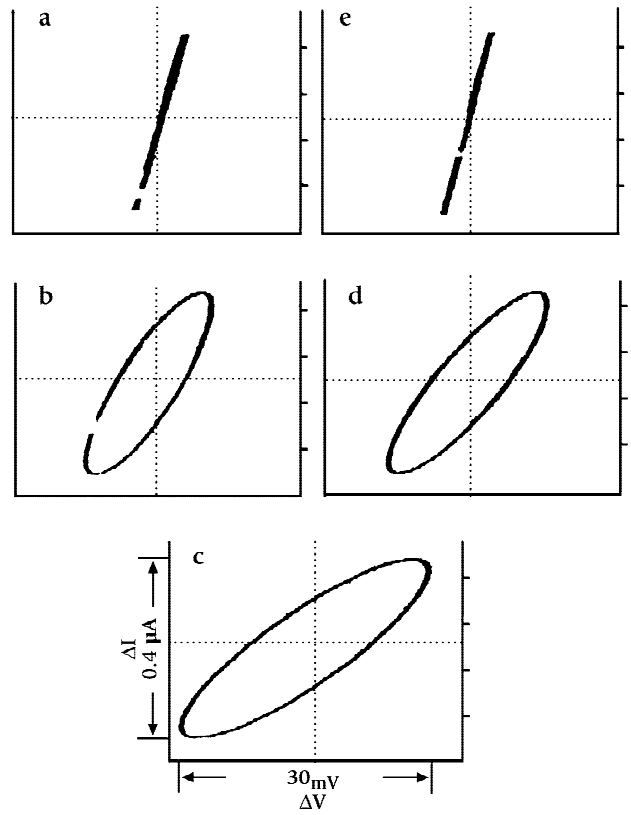

Figure 5. Typical ΔI(ordinate)/ΔV(abscissa) ellipses in response to the symmetric sinusoidal currents (30 Hz, 4×10^{-7} amps) recorded at positions **a, b, c, d,** and **e**. No significant phase difference was seen in either positions **a** or **e**. The slopes of **a** and **e** correspond to the series resistance *Rs*. At position **b, c,** and **d** significant phase differences can be seen.

If a symmetric sinusoidal current is injected between the upper and lower pools, Δi/Δv ellipse can be observed on the oscilloscope. This ellipse enables us to estimate not only the value of Cm but also the phase difference between Δi and Δv by the equations shown in Figure 2b (Kishimoto 1974) in which the absolute value of the impedance is equal to Δv/Δi. On the other hand, the phase angle (Θ) of the impedance is related to M (=Δi; the amplitude of the injected sinusoidal current) and N in Figure 2b by the equation: $\sin^{-1}\Theta = N/M$.

Chara corallina plant material was grown in a soil-extract culture medium at room temperature, 23 ± 2°C under fluorescent illumination with a dark and light period of 12 h and pH of 8.0. A pair of internodes (internode A, 50 ± 10 mm; internode B, 37 ± 4 mm in length; 800 ± 100 μm in diameter) joined by a node-complex was isolated from the plant. At both ends of the material, the node complexes, N_a and N_b, remained. In the nodal-complex, a single cell layer composed of two central nodal cells, Nc, is surrounded by seven large nodal-complex-cells, first-peripheral-nodal cells, developed from Nc (Iwasaki 1962), so that no primer cytoplasmic-junction should exist between the internode and these surrounding cells, but between Nc and internode, as plasmodesmata (Figure 3). Electrical potential changes of one of the water-films that was on the nodal complex mainly corresponded to that of Nc because the relative current density through this part was 10 times larger than that through the other part of the internode. That is, the potential change measured at position b corresponded to that at the interface between internode A and Nc. The potential change at position d corresponded to that at the Nc/internode B interface. In other words, scanning of the electrode unit enabled us to distinguish the elec-

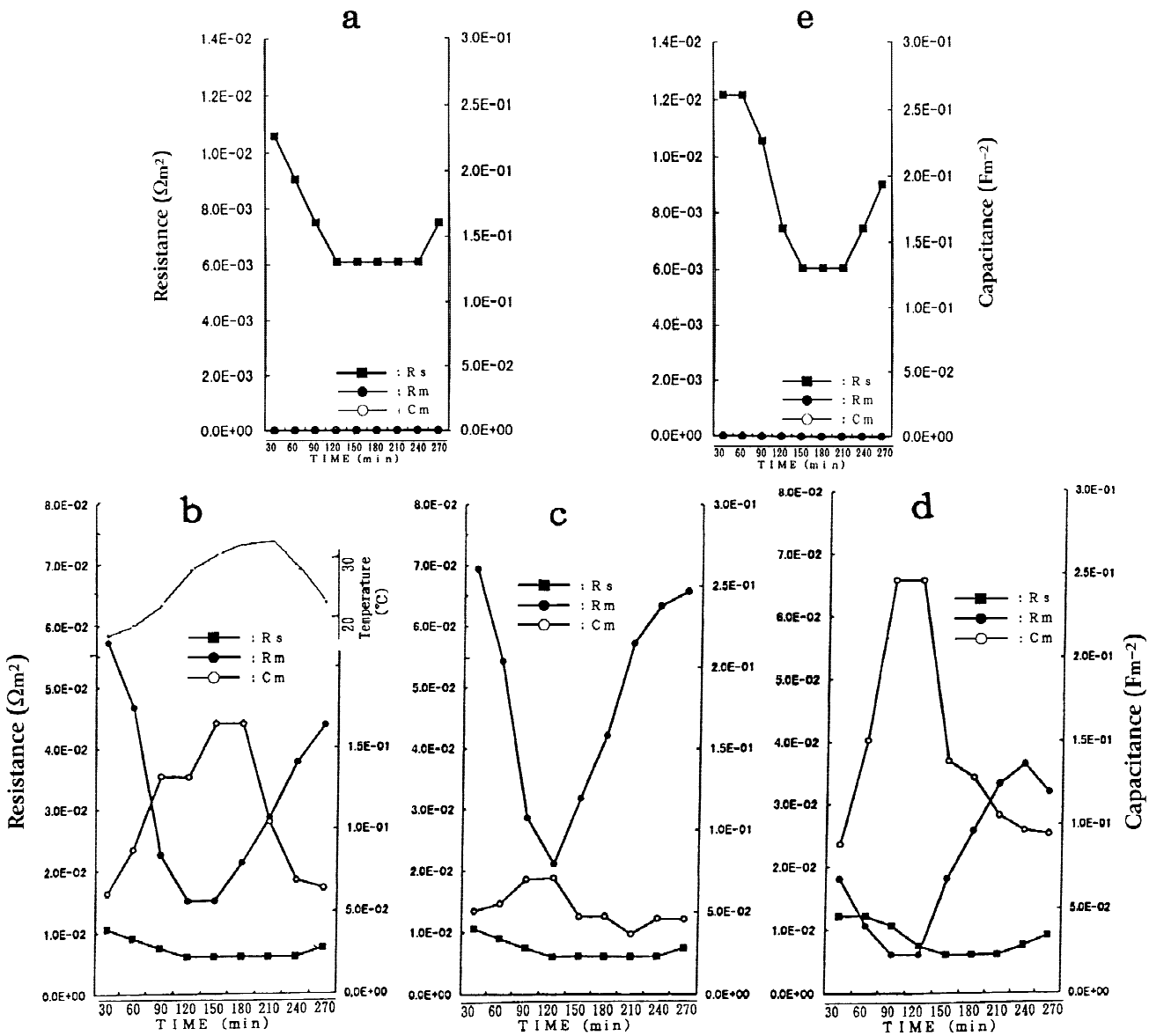

Figure 6. Influence of temperature on Rs, Rm, and Cm at positions **a**, **b**, **c**, **d**, and **e**. Values of Rs, Rm, and Cm are plotted as a function of time. Temperature change is indicated at the top of **b**. Scales on the left and right indicate resistance (Ωm^2) and capacitance (Fm^{-2}), respectively.

trical properties of closely spaced individual interfaces (10 μm apart) without any unfavorable mechanical stimulus to the material.

Before the experiment, a pair of internodes was preincubated in APW under the same conditions as for plant culture. The six leaflets and many smaller basal nodal cells surrounding the node complex were carefully removed as much as possible with a pair of tweezers with fine tips under a dissecting microscope. The seven first-peripheral-nodal cells remained intact.

This technique with an external measurement in a moist chamber overcame unfavorable mechanical and physiologic disturbances expected for long-term measurements with conventional intracellular glass micropipette electrodes.

Results and Discussion

Figure 4 shows typical electrical potential change (ΔV) data at positions of a, b, c, d, and e indicated in Figure 3 in response to a constant square current (ΔI 30 Hz, 4×10^{-7} amp, symmetric pulses including a fast time constant of less than 0.5 ms) given between the upper and lower regions of material. At positions

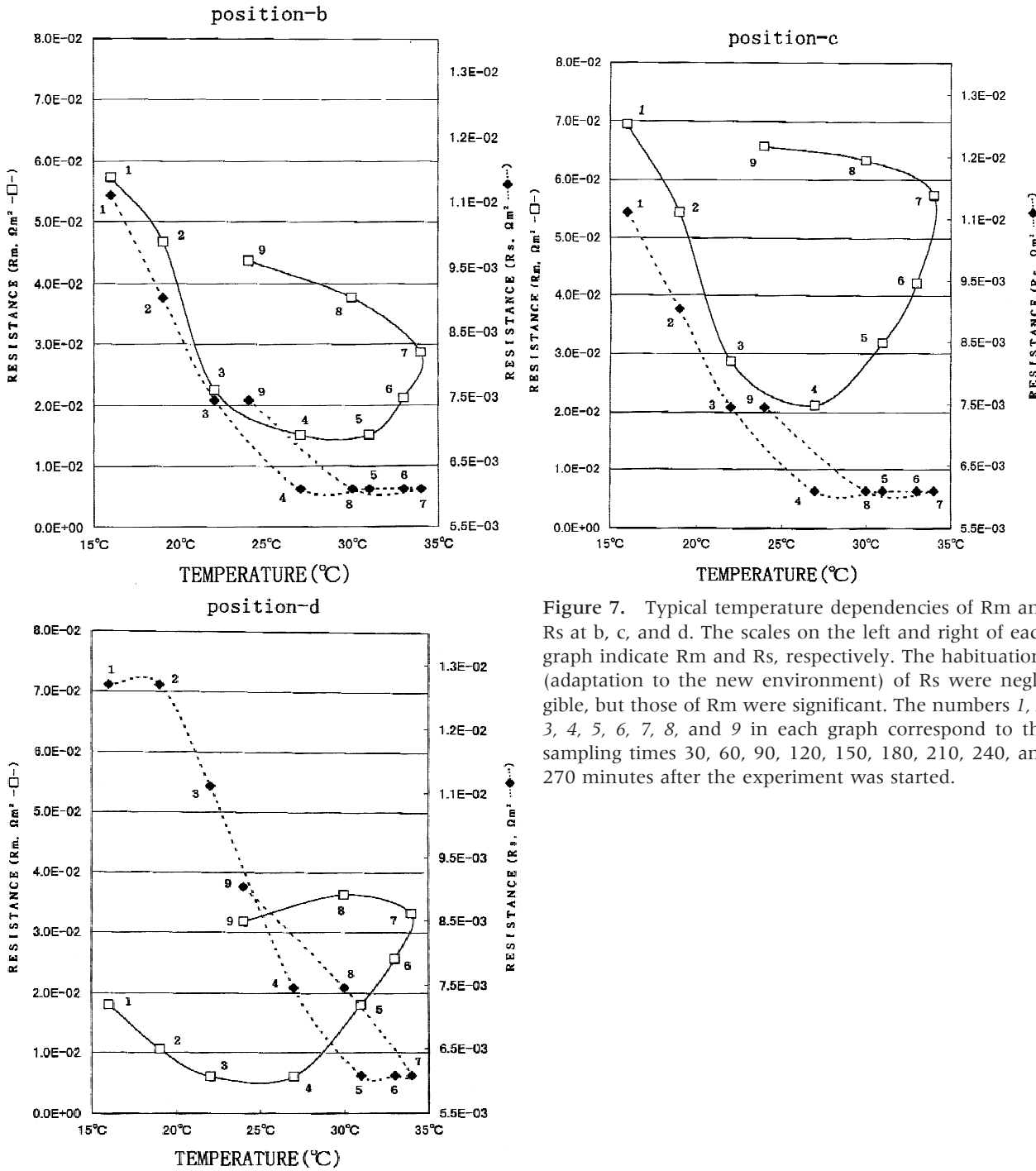

Figure 7. Typical temperature dependencies of Rm and Rs at b, c, and d. The scales on the left and right of each graph indicate Rm and Rs, respectively. The habituations (adaptation to the new environment) of Rs were negligible, but those of Rm were significant. The numbers *1, 2, 3, 4, 5, 6, 7, 8,* and *9* in each graph correspond to the sampling times 30, 60, 90, 120, 150, 180, 210, 240, and 270 minutes after the experiment was started.

a and b, negligible capacitative components were observed, but the resistive components were significant, corresponding to Rs in the equivalent circuit. Furthermore, the value of Rs observed was equivalent to the resistance of aqueous electrolyte solution with the ionic strength of roughly 200 mM. On the other hand, at positions b, c, and d significant τs of 3 $\times 10^{-3}$, 1.5 $\times 10^{-3}$, and 2 $\times 10^{-3}$ s, respectively, were observed. This suggested that some leaky electrical capacitative components existed at these positions corresponding to both the interfaces between internode A and B and the Nc and to the values across the nodal complex-cells. This response corresponded to the Rm and the Cm. Thus, Rs, Rm, and Cm can be calculated by the equations: Vs/I = Rs, Vm/I = Rm, τ = Rm × Cm. Figure 5 shows the $\Delta I/\Delta V$ ellipses of the data of Figure 4.

Figure 6 shows the time dependencies of Rm, Rs,

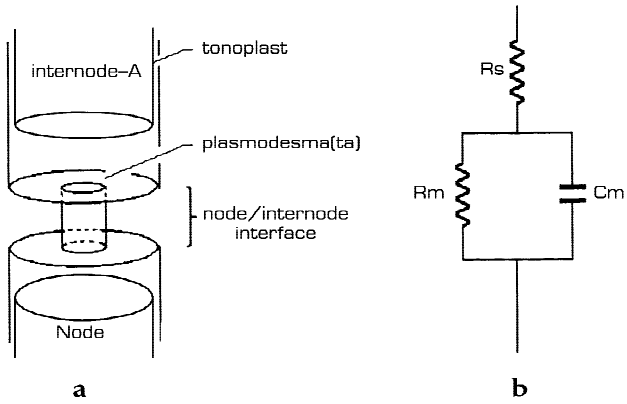

Figure 8. **(a)** Schematic diagram of the structure of the interface between node and internode A. The sum of plasmodesmata is represented by the central cylinder. The bold lines correspond to the plasmalemma. **(b)** Electrical equivalent circuit of the interface. Rs, Rm, and Cm correspond mainly to the electrical resistance component in the vacuole, in the cylinder of plasmodesmata (including tonoplast in series), and in the capacitance component of a double layer of plasmalemma. The resistance and capacitance components for the tonoplast are included in the circuit because the design does not resolve the contribution of the tonoplast.

and Cm with change in temperature. Rs at the positions of a, b, c, d, and e decreased and then increased in phase with the rise and decline in temperature. These responses of Rs showed the same temperature dependency as those of an aqueous electrolyte solution with an ionic strength of 200 mM. Data from positions at a and e are magnified to emphasize the responses. The temperature coefficient, Q_{10}, of Rs was smaller than 2. The responses of Rm at the positions of b, c, and d also decreased with the initial rise in temperature but later increased, although the temperature was still rising. The responses of Cm at those positions showed the same time dependencies as those of Rm but increased with a rising temperature. The temperature coefficient, Q_{10}, of Rm and Cm was larger than 2.5. The large Q_{10} suggests that some physiologic mechanism must be responsible for the control of the electrical properties at those particular regions. The apparent resistance (Rm_c) and capacitance (Cm_c) at position c was approximately the sum of values at b and d, namely $Rm_c = Rm_b + Rm_d$, $Cm_c = 1/(1/Cm_b + 1/Cm_d)$. Furthermore, the double-water-film electrode technique enabled us to distinguish the electrical characteristics of individual interfaces, internode A/Nc and Nc/internode B, spaced closer than 20 μm of one another. The structures of those interfaces were intact; no cell was impaled.

Figure 7 shows the influence of temperature change on Rm and Rs at positions b, c, and d. The habituations of Rs were negligible, but those of Rm were significant. It was clearly suggested again that a dynamic homeostatic control mechanism was independently operating at both interfaces where a number of plasmodesmata have been observed by electron microscopy. Although the effective electrical current density across the tonoplast is unknown because the given current propagates through not only the vacuole but also the cytoplasm, it is worth noting the correlation between the electrical properties and the structure around the node/internode interface. Figure 8 shows a schematic diagram of the interface with the total openings of the plasmodesmata and an electrical equivalent circuit for this region. Rs and Rm correspond mainly to the resistance components of the vacuole and the openings of all plasmodesmata, respectively (including tonoplast in series). Cm corresponds to the capacitance component of two layers of plasmalemma (including tonoplast in series). Because the leakage current through the plasmalemma is 500 times smaller than that of plasmodesmata and negligible (Spanswick and Costerton 1967), the resistance component of plasmalemma is omitted from the circuit.

The resistance of a cylinder 8×10^{-4} m in diameter and 1×10^{-2} m in length filled with 100 mM of KCl aqueous solution was $1 \times 10^{4}\Omega$ (at 20°C). Assuming the resistance of an average plasmodesma to be $2.6 \times 10^{9}\Omega$, the number of plasmodesmata at the interface between the internode and the central node cells was calculated at 2.6×10^{5}.

Values of $8 \times 10^{-3}\Omega$ m^2 for Rs and $30 \pm 5 \times 10^{-3}$ Ω m^2 for Rm observed with the newly developed double-water-film-electrode were roughly consistent with those observed with ordinary techniques using intracellular glass micropipette electrodes. Furthermore, the calculated capacitance of 1.5 ± 10^{-1} Fm^{-2} for Cm was consistent, if we assume that 0.5–1% total area of plasmalemma was occupied with plasmodesmata at the mature node/internode interface of *Chara*. It would be reasonable to assume that some effective area of the interface was occupied with a certain number of immature plasmodesmata that did not completely pass through the cell wall at the node/internode interface, but that could be controlled by some mechanism as pre-existing primer plasmodesmata. The number of plasmodesmata was the same as the value estimated from electron micrographs (Picket-Heaps 1967; Spanswick and Costerton 1967).

These consistencies strongly suggest that the double-water-film electrode technique is useful for electrophysiologic studies on the interface between node and internode. The technique permits more

quantitative results and enables us to perform experiments concerned with the turgor pressure gradient on Rs, Rm, and Cm.

ACKNOWLEDGMENTS

The author dedicates this article to the late Dr. Paul Barnett Green, who was not only his supervisor in the graduate school at the University of Pennsylvania but also one of the few persons among those he has met who can be called a humanitarian.

The author is grateful to Drs. U. Kishimoto (honorary professor of Osaka University), K. Kuroda (honorary associate professor of Osaka University), T. Shimmen (Univ. Himeji Tec.), and T. Maki and M. Nakano (Univ. Occupl. and Envl. Health) for their critical and helpful comments on this work. The author expresses many thanks to Ms. N. Sakai and T. Mochinaga for their constant assistance.

REFERENCES

Chilcott TC. 1988. Admittance tomography of *Chara corallina:* a study of the electrical spatial structures associated with photosynthesis. PhD dissertation. University of New South Wales, Australia.

Chilcott TC, Coster HGL, Ogata K, Smith JR. 1983. Spatial variation of the electrical properties of *Chara australis* II membrane capacitance and conductance as a function of frequency. Aust J Plant Physiol 10:353–362.

Chilcott TC, Lucas WJ, Coster HGL, Francesche VR. 1993. Impedance spectroscopy studies on plasmodesmata in *Chara*, in model systems for studying cell motility and membrane transport. Proceeding of the symposium honoring the *80th* birthday of Prof. N. Kamiya, Giant cells of the Characeae, pp 61–62.

Coster HGL, Chilcott TC, Ogata K. 1984. Fluctuations in the electrical properties of *Chara* and the spatial structure of the electro-chemical characteristics. In: Lucas WJ, Berry JA (eds) Inorganic carbon uptake by aquatic photosynthetic organisms. American Society of Plant Physiologists, pp 255–269.

Côté R, Thain JH, Fensom DS. 1986. Increase in electrical resistance of plasmodesmata of *Chara* induced by an applied pressure gradient across nodes. Can J Bot 65:509–511.

Ding D-Q, Tazawa M. 1989. Influence of cytoplasmic streaming and turgor pressure gradient on the transnodal transport of rubidium and electrical conductance in *Chara corallina.* Plant Cell Physiol 20:739–748.

Franceschi VR, Lucas WJ. 1982. The relationship of the charosome to chloride uptake in *Chara corallina:* physiological and histochemical investigations. Planta 164:172–178.

Green PB. 1968. Growth physics in *Nitella:* a method for continuous in vivo analysis of extensibility based on a micromanometer technique for turgor pressure. Plant Physiol 43: 1169–1184.

Iwasaki N. 1962. Wntwicklungsgeschichtliche Untersuchungen an den Characeen. II. *Chara benthamii.* Bot Mag Tokyo 75:1–9.

Kikuyama M, Hara Y, Shimada K, Yamamoto K, Hiramoto Y. 1992. Intercellular transport of macromolecules in *Nitella.* Plant Cell Physiol 33:413–417.

Kishimoto U. 1974. Transmembrane impedance of the *Chara* cell. Jap J Physiol 24:403–417.

Lucas WJ, Ogata K. 1985. Hydroxyl and bicarbonate associated transport processes in *Chara corallina;* studies on the light-dark regulation mechanism. J Exp Bot 36:1947–1958.

Ogata K. 1983. The water-film electrode: a new device for measuring the Characean electro-potential and—conductance distributions along the length of internode. Plant Cell Physiol 24: 695–703.

Philippson M. 1921. Les lois de las resistance electrique des tissues vivants. Bull Acad Roy Belg Clin Sci 7:387–403.

Pickett-Heaps JD. 1967. Ultrastructure and differentiation in *Chara* sp. Aust J Biol Sci 20:539–551.

Robards AW, Lucas WJ. 1990. Plasmodesmata. Plant Physiol 41: 369–419.

Shibaoka T, Tabata T. 1981. Electrotonic coupling between adjacent internodal cells of *Chara braunii:* transmission of action potential beyond the node. Plant Cell Physiol 22:397–411.

Spanswick RM, Costerton JWF. 1967. Plasmodesmata in *Nitella translucens:* structure and electrical resistance. J Cell Sci 21:451–464.